UDK 621.355:581.143.5
Original scientific article/Izvirni znanstveni članek

ISSN 1580-2949
Mater. Tehnol.

RESYNTHESIS AND ELECTROCHEMICAL PERFORMANCE OF NCM111 USING ULTRASOUND-ASSISTED LEACHATE FROM SPENT LITHIUM-ION BATTERY CATHODES

PONOVNA SINTEZA IN ELEKTROKEMIJSKE LASTNOSTI NCM111 IZ ULTRAZVOČNO PRIDOBLJENE LUŽNE RAZTOPINE IZTROŠENEGA LITIJ-IONSKEGA MATERIALA ZA BATERIJE

Honghao Yu, Junhui Ye, Nianping Li, Xin Li*

[1]School of Materials Science and Engineering, Shenyang Ligong University, Shenyang, Liaoning 110159, China

Prejem rokopisa – received: 2025-04-30; sprejem za objavo – accepted for publication: 2025-08-28

doi:10.17222/mit.2025.1431

The widespread use of lithium-ion batteries (LIBs) led to a substantial accumulation of spent cathode materials, creating an urgent need for environmentally sustainable recycling methods that address both ecological concerns and the recovery of critical metals. A novel strategy integrating ultrasound-assisted deep eutectic solvent (DES) leaching and urea-assisted co-precipitation for the regeneration of high-performance $LiNi_1/_3Co_1/_3Mn_1/_3O_2$ (NCM111) cathodes from spent $LiCoO_2$ was developed. The results revealed that the transition metal-to-urea molar ratio critically governs the structural and electrochemical properties of regenerated materials. An NCM111 sample with an optimized transition metal-to-urea ratio of 1:2 had an ordered layered structure (I(003)/I(104) = 1.336), uniform spherical secondary particles (1–3 μm), and minimal cation mixing. These structural advantages translated into exceptional electrochemical performance, including an initial Coulombic efficiency of 84.84 %, 96.13 % capacity retention after 30 cycles, low charge-transfer resistance (37.26 Ω), and enhanced redox reversibility (ΔE_p = 0.21 V). Electrochemical impedance spectroscopy (EIS) and cyclic voltammetry (CV) further confirmed the superior interfacial kinetics and reaction reversibility of the optimised sample.

Keywords: spent lithium-ion batteries, ultrasound-assisted leachate, resynthesis, deep eutectic solvent, $LiNi_{1/3}Co_{1/3}Mn_{1/3}O_2$

Zelo velika uporaba litij-ionskih baterij (LIBs; angl.: lithium-ion batteries) je povzročila kritično kopičenje iztrošenih katodnih materialov. To je zahtevalo razvoj metodologije okolju prijaznega recikliranja, tako glede ekoloških standardov, kot tudi rešitev za ponovno pridobivanje strateških kovin. Avtorji v pričujočem članku opisujejo novo strategijo in razvoj integriranega z ultrazvokom podprtega globokega evtektskega raztopnega (DES; angl.: deep eutectic solvent) jedkanja s sečnino podprto ko-prepitacijo (so-izločanje) za regeneracijo visoko zmogljivih $LiNi_{1/3}Co_{1/3}Mn_{1/3}O_2$ (NCM111) katod iz iztrošenega $LiCoO_2$. Rezultati raziskave so pokazali, da molsko razmerje med prehodnimi kovinami in sečnino kritično vpliva na strukturne in elektro-kemijske lastnosti regeneriranih materialov. Vzorci NCM111 z optimiziranim razmerjem med prehodnimi kovinami in sečnino (1:2) imajo urejeno plastovito strukturo (I(003)/I(104) = 1,336, enovite kroglične delce (velikosti od 1 μm do 3 μm) in minimalno kationsko mešanje. Te strukturne prednosti so se odrazile v izjemni elektrokemični zmogljivosti, vključno z začetnim 84,84 %-nim Coulombovim izkoristkom, 96,13 %-no ohranitvijo kapacitete po 30-tih ciklih, majhno upornostjo prenosa naboja (37,26 Ω) in izboljšano redoks reverzibilnostjo (ΔE_p = 0,21V). Elektrokemijska impedančna spektroskopija (EIS; angl.: Electrochemical Impedance Spectroscopy) in ciklična voltametrija (CV; angl.: Cyclic Voltammetry) sta nadalje potrdili vrhunsko medmejno kinetiko in reverzibilnost reakcije optimiziranih preizkušancev.

Ključne besede: izrabljene litij-ionske baterije, regeneracija, asistenca (pomoč) ultrazvoka, ponovna sinteza (predelava), globoka evtektična raztopina, $LiNi_{1/3}Co_{1/3}Mn_{1/3}O_2$

1 INTRODUCTION

Lithium-ion batteries (LIBs) have become the cornerstone of modern energy storage systems, powering portable electronics and electric vehicles owing to their high energy density, lack of memory effect, and excellent thermal stability.[1] With the rapid growth of the electric and hybrid vehicle markets, the global demand for LIBs is projected to surge from 700 GWh in 2022 to over 4.7 TWh by 2030, according to McKinsey's battery report.[2] Over the next five years, a dramatic increase in discarded lithium-ion batteries is expected, examples being the widespread use of electric vehicles since 2018. Valued at over $100 billion, the recycling market for these batteries has appeared.[3] Evident from current recycling practices, numerous spent LIBs may end up improperly processed in coming years. Not only does this represent resource wastage, but also poses significant environmental risks. Presently inadequate battery recycling systems fail to handle the impending surge, highlighting both material loss and ecological hazards. Projected figures suggest an alarming accumulation of unrecycled units, with consequences extending beyond mere financial metrics. Already observable are the strains on existing infrastructure, pointing toward unsustainable trajectories unless interventions occur. Moreover, the disposal of spent lithium-ion batteries (LIBs) presents substantial environmental and economic challenges for the recycling

*Corresponding author's e-mail:
lx80ws@126.com (Xin Li)

industry. These batteries contain elevated concentrations of toxic heavy metals, such as cobalt, manganese, nickel, and lithium, which may severely threaten ecosystems and human health if improperly managed – particularly given the increasing volumes of discarded lithium cobalt oxide ($LiCoO_2$) batteries.[4] Conversely, these metals constitute valuable resources, with higher purity and concentration in spent LIBs than in natural ores. Thus, recycling serves not only as an environmental imperative but also as an economically viable strategy for resource recovery.

Numerous methods have been reported in the literature for processing spent lithium-ion battery (LIB) cathode materials to recover their constituent metals.[5–12] Among these, hydrometallurgical processes are the most widely adopted recycling method. These methods typically employ inorganic acids, organic acids, or deep eutectic solvents to dissolve active cathode materials.[13–15] Subsequent purification steps, such as solvent extraction and chemical precipitation, are used to isolate valuable metals. However, the separation of metals with similar chemical properties often requires complex, multi-stage processes, leading to increased costs and energy consumption.

Recent advances have focused on the direct regeneration of cathode materials using leaching solutions. For instance, Zhang et al. successfully resynthesised $LiNi_{1/3}Co_{1/3}Mn_{1/3}O_2$ using sol-gel methods, achieving excellent reversible capacity and cycling stability.[16] Similarly, Luo and Wang demonstrated that co-precipitation of $Ni_{1/3}Co_{1/3}Mn_{1/3}(OH)_2$ precursors from acid leachates could be used to regenerate high-performance $LiNi_{1/3}Co_{1/3}Mn_{1/3}O_2$ (NCM111) cathodes materials.[17] Alternative hybrid approaches that combine hydrometallurgy with solid-state synthesis have also shown promise. Zhuang and Sun, for example, recovered Co_3O_4 and Li_2CO_3 from spent $LiCoO_2$ cathodes and subsequently regenerated $LiCoO_2$ through ball milling and calcination.[18]

In this study, we present a novel recycling strategy for spent lithium cobaltate ($LiCoO_2$) cathodes. Our approach utilises ultrasound-assisted deep eutectic solvent leaching to obtain a lithium- and cobalt-rich solution.[19] This solution was then used to synthesise NCM111 precursors via a urea-assisted hydrothermal method, with a systematic investigation of the effects of urea concentration on the properties of NCM111. Finally, the precursor was combined with Li_2CO_3 recovered from the filtrate and calcined to produce a high-quality NCM111 cathode material.

2 EXPERIMENTAL PART

2.1 Materials and reagents

Spent LIBs were provided by Jiangsu Funeng Lithium Battery Co., Ltd. The cathode materials were manually disassembled, and the surface binders and residual electrolytes were removed via thermal treatment at 400 °C for 2 h in air. Choline chloride (ChCl, ≥98.0 %) was purchased from Macklin Biochemical Co., Ltd. Ethylene glycol (EG, AR grade) and urea (AR grade) were obtained from Tianjin Damao Chemical Reagent Factory. Manganese (Mn), lithium (Li), nickel (Ni) and cobalt (Co) were supplied as chloride salts by Tianjin Damao Chemical Reagent Factory. All chemicals were used as received without further purification, and deionised water was used in all experiments.

2.2 Leaching of spent $LiCoO_2$

The deep eutectic solvent (DES) was prepared by mixing choline chloride (ChCl), ethylene glycol (EG), and benzoic acid (BA) in a molar ratio of 1:1.6:1.4, as determined through preliminary optimization experiments. The mixture was heated to 80 °C in a water bath under continuous magnetic stirring until a homogeneous transparent liquid was formed. Leaching experiments were performed in a 150 mL three-neck Pyrex reactor equipped with an ultrasonic probe and an oil bath for precise temperature control.

2.3 Resynthesis of NCM111 with different urea dosages

The NCM111 precursor was synthesised using a urea-assisted co-precipitation method. Stoichiometric amounts of $Ni(CH_3COO)_2{\cdot}4H_2O$ and $Mn(CH_3COO)_2{\cdot}4H_2O$ were added to the leachate to achieve a Ni:Co:Mn molar ratio of 1:1:1. Urea was then introduced as a precipitating agent at different molar ratios relative to transition metal ions (1:1, 1:2, 1:3, and 1:4). The mixture was transferred to a 100 mL Teflon-lined autoclave and maintained at 180 °C for 24 h. The resulting precipitate was filtered, washed with deionised water, and dried overnight at 80 °C.

The obtained precursors were thoroughly mixed with Li_2CO_3 (5 % excess) and subjected to a two-step calcination process: pre-calcination at 500 °C for 6 h, followed by high-temperature treatment at 850 °C for 12 h in a muffle furnace (heating rate: 5 °C/min). The final products were labelled RNCM-1 to RNCM-4, corresponding to increased urea ratios.

2.4 Material characterization

A morphological analysis was performed using field-emission scanning electron microscopy (FE-SEM, Thermo Scientific Apreo 2C) at an acceleration voltage of 3 kV. Phase identification and crystallinity were examined with X-ray diffraction (XRD, Rigaku Ultima IV) with Cu Kα radiation (λ = 0.15406 nm) operating at 40 kV and 40 mA. XRD patterns were recorded in a 2θ range of 10–90° at a scan rate of 10°/min.

2.5 Electrochemical performance

Electrode slurries were prepared by mixing the regenerated NCM111 material, acetylene black, and polyvinylidene fluoride (PVDF) binder in an 8:1:1 weight ratio, using N-methyl-2-pyrrolidone (NMP) as the solvent. The homogeneous slurry was applied onto aluminium foil and dried at 120 °C under vacuum for 12 h. CR2032 coin cells were assembled in an argon-filled glovebox (H_2O < 0.5 ppm, O_2 < 0.5 ppm) using lithium as the counter/reference electrode and 1 M $LiPF_6$ in EC/EMC/DMC (1:1:1 v/v) as the electrolyte. The charge–discharge cycle, and rate tests of the cells were performed on a CT2001A land tester between 2.8 V and 4.4 V at various C-rates (1C = 200 mA/g). Cyclic voltammograms (CVs) and electrochemical impedance spectroscopy (EIS) were recorded using a CHI604D electrochemical workstation. The CVs were tested at 0.1 mV s^{-1} between 2.8 V and 4.4 V, while EIS was tested in a frequency range from 100 kHz to 0.01 Hz with a 5-mV amplitude.

3 RESULTS AND DISCUSSION

3.1 Metal recovery

Figure 1 shows the cobalt leaching efficiencies as a function of the leaching time (5–180 min) and temperature (100–180 °C) under optimised conditions (ChCl:EG:BA = 1:1.6:0.4, solid/liquid ratio = 5 g/L, ultrasonic power = 600 W). Experimental results demonstrated that both the reaction temperature and time significantly influenced the leaching efficiency, with higher temperatures and longer times leading to markedly improved leaching efficiency. Specifically, the highest leaching efficiency was observed at 180 °C, achieving 98.48 % within 60 min and nearly complete leaching (99.99 %) after 90 min. In contrast, significantly lower leaching rates were obtained at 100 °C and 140 °C, reaching only 26.73 % and 76.46 %, respectively, after 180 min.

This pronounced temperature and time dependence clearly demonstrates the thermally activated nature of the leaching process, where optimal conditions for efficient cobalt recovery from spent lithium-ion battery cathodes were achieved at 180 °C and 60 min. These findings establish critical process parameters for maximising metal recovery efficiency while minimising the energy consumption and processing time.

3.2 Characterization of regenerated NCM111

The structural characteristics of NCM111 cathode materials synthesised using different transition metal-to-urea molar ratios were investigated with XRD. As shown in **Figure 2**, the XRD patterns of all the synthesised samples exhibit well-defined diffraction peaks that match the characteristic α-$NaFeO_2$ layered structure (space group R-3 m) when compared with the standard $LiNiO_2$ reference pattern (PDF#09-0063).[20] The intensity ratio of the (003) to (104) diffraction peaks (I(003)/I(104)) for the NCM111 sample was quantitatively analysed, as this parameter serves as a sensitive indicator of cation ordering, specifically reflecting the degree of Ni^{2+}/Li^{+} cation mixing in the layered oxide framework. As shown in **Table 1**, the sample prepared with the transition metal-to-urea ratio of RNCM-2 exhibited the most desirable structural characteristics, as reflected by its I(003)/I(104) ratio of 1.336. This value significantly exceeds the threshold ratio of 1.2, which is typically associated with optimal electrochemical performance in layered cathode materials.[20] The enhanced structural ordering in the RNCM-2 sample directly correlates with its improved electrochemical properties, including superior cycling stability, enhanced rate capability, and higher energy density.

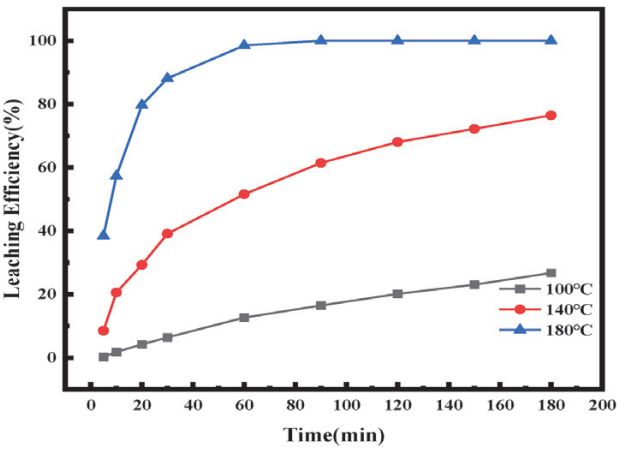

Figure 1: Effect of leaching time and temperature on leaching of Co (ChCl:EG:BA = 1:1.6:0.4, solid/liquid ratio = 5 g/L, ultrasonic power = 600 W)

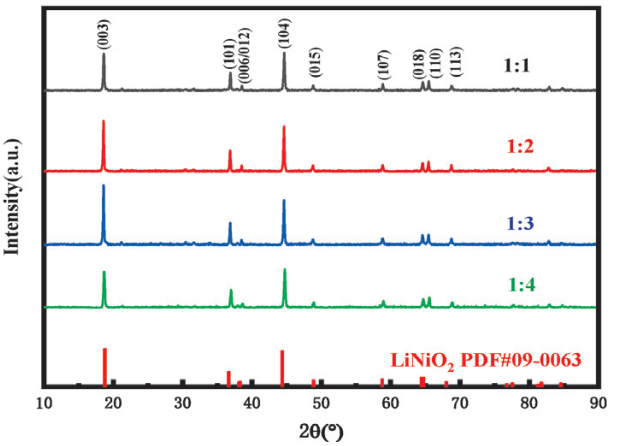

Figure 2: XRD patterns of regenerated NCM111

Table 1: Relative peak intensity ratios (I003/I104) for NCM111 materials prepared with different transition metal (Ni,Co,Mn):urea molar ratios

Transition metal (Ni,Co,Mn):urea molar ratio	Denominations	I(003)	I(104)	I(003)/I(104)
1:1	RNCM-1	2401	2147	1.11830
1:2	RNCM-2	2833	2121	1.33569
1:3	RNCM-3	1588	1639	0.96888
1:4	RNCM-4	995	958	1.03862

Morphological characterization obtained with SEM (**Figure 3**) provides further insight into the microstructure-property relationships. All samples exhibited spherical secondary particle morphologies; however, the RNCM-2 sample demonstrated significantly improved morphological characteristics. Specifically, the sample exhibited a narrower particle size distribution, centred at 1–3 μm in diameter, more uniform surface topography, better particle dispersion, and enhanced structural homogeneity throughout the material. These favourable morphological features are expected to facilitate a more efficient charge transport and a more uniform current distribution during electrochemical cycling.

In contrast, the sample prepared with the RNCM-1 transition metal-to-urea ratio exhibited less desirable morphological characteristics, including irregular particle shapes, increased surface roughness, and a broader size distribution. Such morphological imperfections may lead to several detrimental effects on electrochemical performance, including elevated interfacial resistance, non-uniform current distribution, hindered lithium-ion diffusion kinetics, and compromised structural integrity during prolonged cycling.

The comprehensive structural and morphological characterization presented here conclusively demonstrates that precise control of the transition metal-to-urea molar ratio during synthesis, particularly the optimal RNCM-2 ratio, enables the fabrication of NCM111 with both superior crystallographic ordering and an ideal particle morphology.

Figure 3 reveals significant differences in the morphology and homogeneity between the samples (RNCM-1, RNCM-2, RNCM-3 and RNCM-4), with RNCM-4 exhibiting inferior structural characteristics. The morphological evolution demonstrates a clear dependence on the urea content, as evidenced by the substantial variations observed with different urea additions. Notably, electrochemistry performance tests establish a direct correlation between improved morphology and enhanced electrochemical properties.

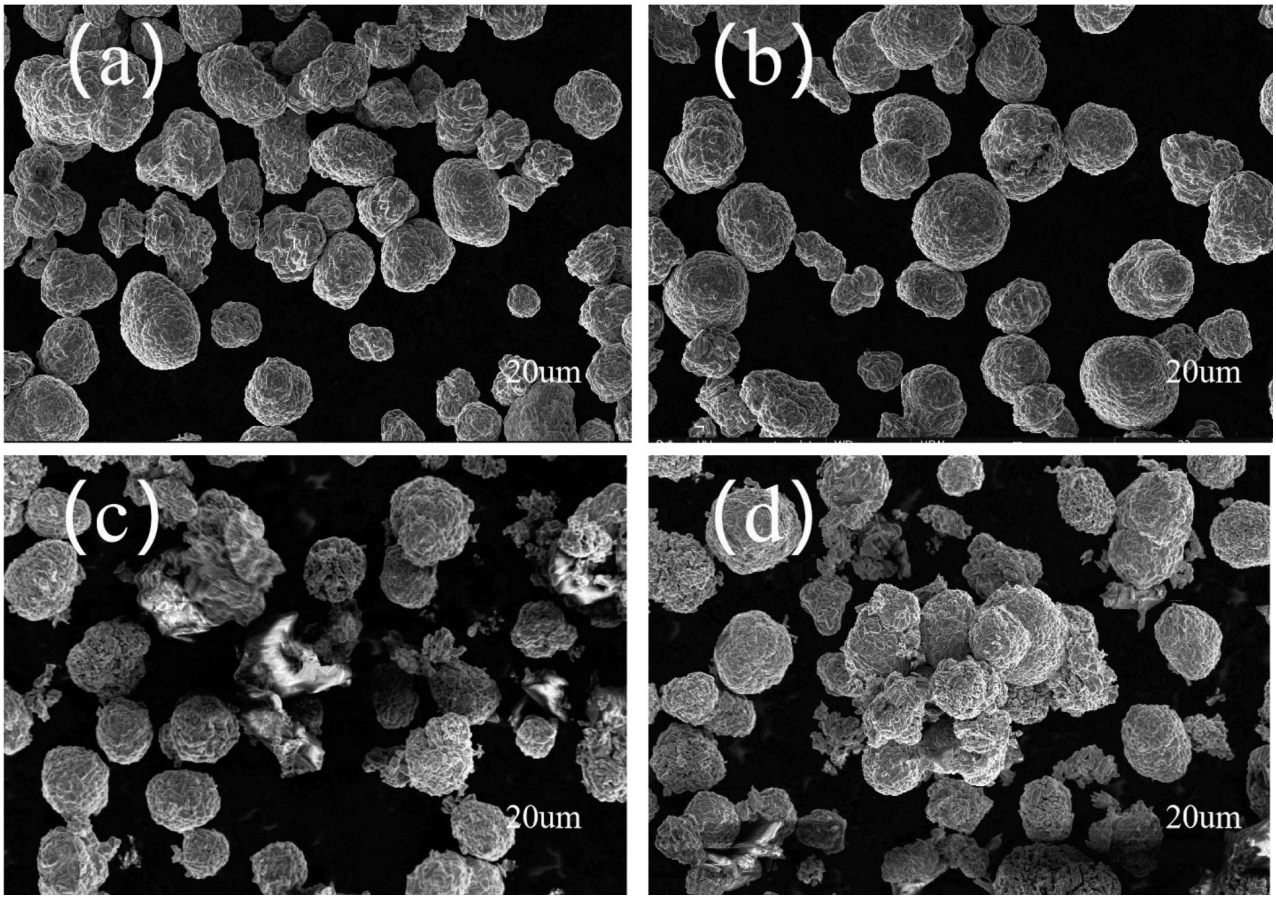

Figure 3: SEM patterns of different ratios of NCM111: a) RNCM-1; b) RNCM-2; c) RNCM-3; d) RNCM-4

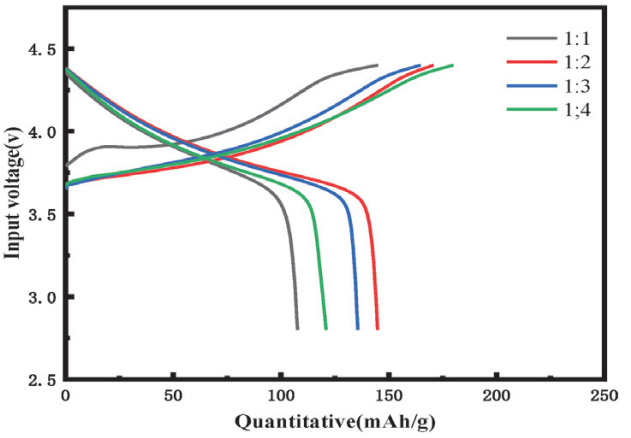

Figure 4: First turn charge/discharge curves

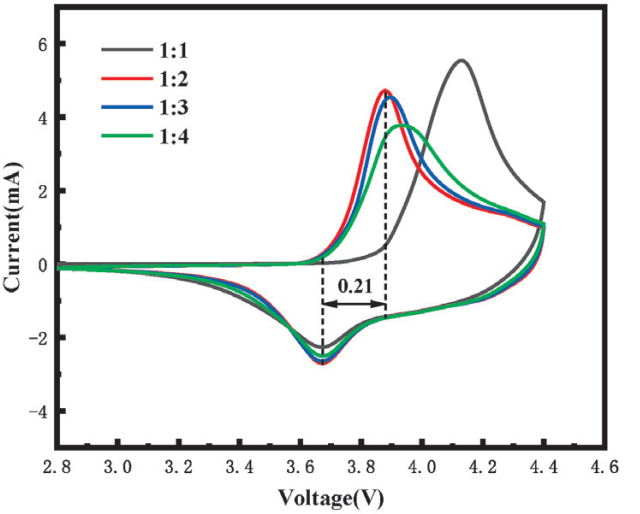

Figure 6: Cyclic voltammetry curves for different transition metal-to-urea molar ratios (1:1,1:2,1:3,1:4)

3.3 Electrochemical properties of NCM111

The electrochemical performance evaluation of NCM111 with varying transition metal-to-urea molar ratios (RNCM-1 to RNCM-4) revealed significant composition-dependent characteristics, as shown in **Figure 4**. Under standard test conditions (0.1C rate, a voltage window of 2.8–4.4 V), the initial charge/discharge capacities demonstrated a clear optimisation at the 1:2 stoichiometric ratio, exhibiting values of 170.7/144.6 mAh·g^{-1}. This represents a substantial improvement compared to other compositions (145/107.7 mAh·g^{-1} for RNCM-1, 164.7/135.6 mAh·g^{-1} for RNCM-3, and 179.9/120.9 mAh·g^{-1} for RNCM-4). The corresponding Coulombic efficiency of the NCM111 sample with the transition metal-to-urea molar ratio of 1:2 followed a similar trend, achieving the highest initial efficiency of 84.84 %, significantly surpassing the other formulations (74.27 % for RNCM-1, 71.28 % for RNCM-3, and 67.17 % for RNCM-4). This superior electrochemical performance can be directly correlated with the enhanced structural ordering, as evidenced by the elevated I(003)/I(104) ratio (1.336).

Figure 5 shows the capacity changes and retention rates of the NCM111 cathode materials with varying ratios during 30 cycles of discharging at 0.1C. Notably, the sample with the RNCM-2 transition metal-to-urea ratio exhibited exceptional cycling performance, maintaining a discharge capacity of 139.2 mAh·g^{-1} and an outstanding capacity retention of 96.13 % after 30 cycles. This remarkable electrochemical stability contrasts with the performance of other compositions (RNCM-1, RNCM-3,

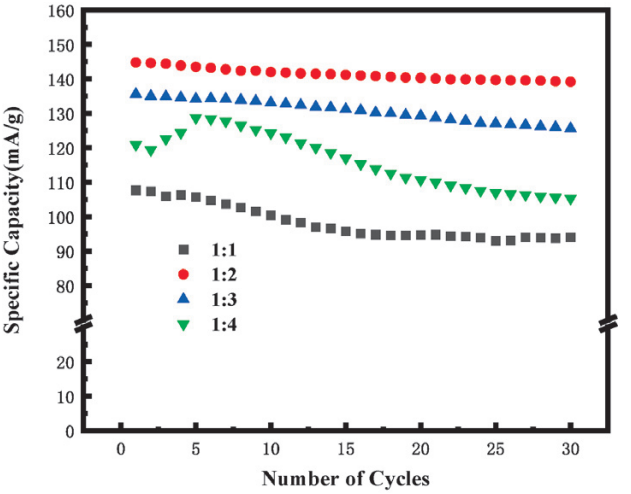

Figure 5: Cycle performance curves

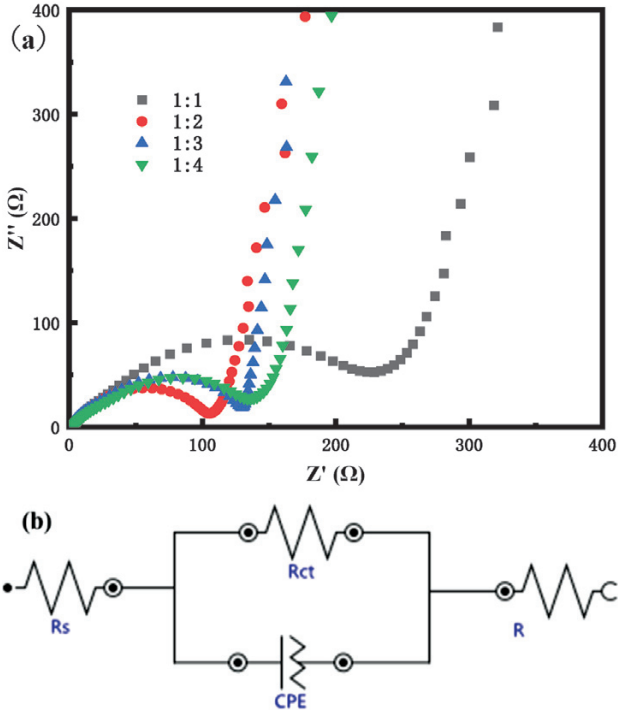

Figure 7: a) Nyquist plot of AC impedance for different transition metal-to-urea molar ratios (1:1,1:2,1:3,1:4,); b) equivalent circuit

and RNCM-4 ratios), which show relatively lower discharge capacities (94, 125.6 and 105.3) mAh g^{-1}, respectively and reduced retention rates (87.28, 92.63 and 87.10) %.

Generally, the intercalation and deintercalation of lithium ions are coupled with the redox reactions of nickel ions, as reflected in the redox peaks of the CV curve. The potential difference (ΔEp) between the anodic and cathodic peaks indicates the reversibility of the electrochemical reaction and degree of electrochemical polarisation. These redox peaks also reveal the extent of phase transformation in the material during the charge/discharge processes. To further analyse the electrochemical behaviour of NCM111 materials with varying ratios of transition metal ions to urea, cyclic voltammetry (CV) curves were measured at a scan rate of 0.4 mV/s within a voltage range of 2.8–4.4 V. As shown in **Figure 6**, the measured CV curves exhibit well-defined redox peaks that correspond to the reversible intercalation/deintercalation of lithium ions coupled with the oxidation/reduction of transition metal cations (Ni^{2+}/Ni^{3+} and Co^{2+}/Co^{3+}). The potential separation (ΔE_p) between the anodic and cathodic peaks serves as a quantitative indicator of electrochemical reversibility, with smaller ΔE_p values signifying lower polarization and more favourable reaction kinetics.[21] Particularly noteworthy is the electrochemical behaviour of the RNCM-2 sample, which demonstrates optimal performance characteristics. This composition exhibits sharply defined redox peaks at 3.88 V (oxidation) and 3.67 V (reduction), and a minimal potential separation of $\Delta E_p = 0.21$ V.

Figure 7 displays the Nyquist plots of the AC impedance for the NCM111 cathode materials at various scales, accompanied by the corresponding equivalent circuit model. The impedance spectra exhibit four characteristic regions: ultra-high frequency (UHF), high frequency (HF), medium frequency (MF), and low frequency. In the equivalent circuit, R_s represents the solution resistance in the high-frequency region, R_{ct} denotes the charge-transfer resistance in the medium-frequency region, and Wt describes the Warburg diffusion impedance of Li ions in the low-frequency region. A constant-phase element (CPE) was incorporated to account for the non-ideal capacitive behaviour of the electrode-electrolyte interface.

As shown in **Figure 7**, all samples demonstrated relatively low electrolyte resistances, suggesting that the electrolyte properties were not the limiting factor for cell capacity degradation. In the intermediate frequency (IF) region, the charge transfer resistance (Rct) exhibited a distinct trend, initially decreasing before increasing as the transition metal ion-to-urea ratio decreased. Notably, a minimum R_{ct} value of 37.26 Ω was achieved for RNCM-2 sample. This observation indicates enhanced electrode reaction kinetics and superior interfacial stability during electrochemical cycling at this specific composition of the electrolyte. In the low-frequency region, the diffusion impedance attained its minimum value at the ratio of RNCM-3, suggesting more favourable Li-ion transport characteristics. Comprehensive analysis revealed that a transition metal ion-to-urea ratio of RNCM-2 represented the optimal composition. The electrode demonstrated a significantly reduced charge transfer impedance, which promoted lithium-ion diffusion within the electrolyte, mitigated electrolyte decomposition, and improved the reversibility and cycling stability of the cathode material. Consequently, the cathode material with this optimal ratio exhibited diminished electrochemical polarisation, lower internal resistance, and enhanced reaction reversibility.

4 CONCLUSIONS

The ultrasound-assisted deep eutectic solvent (DES) leachate derived from spent $LiCoO_2$ cathode materials was demonstrated to function as an efficacious precursor solution for the synthesis of high-performance NCM111 cathode material. In the urea-assisted co-precipitation process, the transition metal-to-urea molar ratio was found to play a critical role in determining the structural and electrochemical properties of the regenerated materials. The RNCM-2 sample with the optimal transition metal-to-urea molar ratio of 1:2 exhibited superior structural characteristics, as evidenced by an ideal layered architecture (I(003)/I(104)), intensity ratio of 1.336 and well-defined spherical secondary particles (1–3 μm in diameter) demonstrating exceptional size homogeneity. These optimised structural attributes were directly correlated with outstanding electrochemical performance, including an initial Coulombic efficiency of 84.84 %, capacity retention of 96.13 % after 30 cycles, and remarkably low charge transfer resistance (37.26 Ω). Further electrochemical characterization revealed enhanced redox reversibility ($\Delta E_p = 0.21$ V) and stable interfacial kinetics in the optimized material. This integrated recycling-regeneration protocol demonstrates three key technological advancements: (i) direct valorisation of DES leachates into functional cathode materials, (ii) precise control of the crystal structure through tailored co-precipitation chemistry, and (iii) establishment of a sustainable circular economy paradigm for lithium-ion battery recycling.

Acknowledgment

The Science and Technology Foundation of Liaoning Province, China (2023-MS-221) Basic Research Projects of the Educational Department of Liaoning Province (JYTMS20230215, LJ212510144031), China.

5 REFERENCES

[1] M. P. Do, J. Jegan Roy, B. Cao, M. Srinivasan, Green Closed-Loop Cathode Regeneration from Spent NMC-Based Lithium-Ion Bat-

teries through Bioleaching, ACS Sustainable Chem. Eng., 10 (**2022**) 8, 2634–2644

[2] Jakob Fleischmann, M. Hanicke, E. Horetsky, D. Ibrahim, S. Jautelat, M. Linder, P. Schaufuss, L. Torscht, A. van de Rijt, Battery 2030: Resilient, sustainable, and circular; McKinsey & Company, 2023

[3] Q. Wei, Y. Wu, S. Li, R. Chen, J. Ding, C. Zhang, Spent Lithium Ion Battery (LIB) Recycle from Electric Vehicles: A Mini Review, Sci. Total Environ., 866 (**2023**), 161380

[4] C. Peng, C. Chang, Z. Wang, B. P. Wilson, F. Liu, M. Lundström, Recovery of high-purity MnO2 from the acid leaching solution of spent Li-ion batteries, JOM, 72 (**2020**) 2, 790–799

[5] P. Meshram, B. D. Pandey, T. R. Mankhand, Extraction of lithium from primary and secondary sources by pre-treatment, leaching and separation: A comprehensive review, Hydrometallurgy, 150 (**2014**), 192

[6] J. Li, X. Li, Y. Zhang, Q. Hu, Z. Wang, Y. Zhou, F. Fu, Trans. Nonferr. Metals Soc. China, 19 (**2009**) 751

[7] S. M. Shin, N. H. Kim, J. S. Sohn, D. H. Yang, Y. H. Kim, Development of a metal recovery process from Li-ion battery wastes, Hydrometallurgy 79 (**2005**),172

[8] C. K. Lee, K. I. Rhee, Preparation of $LiCoO^2$ from spent lithium-ion batteries, J. Power Sources, 109 (**2002**), 17

[9] Y. J. Liu, Q. Y. Hu, X. H. Li, Z. X. Wang, H. J. Guo, Trans. Nonferr. Metals Soc. China, 16 (**2006**), 956

[10] J. F. Paulino, N. G. Busnardo, J. C. Afonso, Recovery of valuable elements from spent Li-batteries, J. Hazard. Mater., 150 (**2008**), 843

[11] P. Meshram, B. D. Pandey, T. R. Mankhand, Hydrometallurgical processing of spent lithium ion batteries (LIBs) in the presence of a reducing agent with emphasis on kinetics of leaching, Chem. Eng. J., 281 (**2015**), 418

[12] D. Mishra, D. J. Kim, D. E. Ralph, J. G. Ahn, Y. H. Rhee, Bioleaching of metals from spent lithium ion secondary batteries using Acidithiobacillus ferrooxidans, Waste Manag., 28 (**2008**), 333

[13] Pratima Meshram, Abhilash, B. D. Pandey, et al., Comparison of Different Reductants in Leaching of Spent Lithium Ion Batteries, JOM, 68 (**2016**) 10, 2613–2623, doi:10.1007/s11837-016-2032-9

[14] Yuanpeng Fu, et al. Effective leaching and extraction of valuable metals from electrode material of spent lithium-ion batteries using mixed organic acids leachant, Journal of Industrial and Engineering Chemistry, 79 (**2019**), 154–162, doi:10.1016/j.jiec.2019.06.023

[15] Pier Giorgio Schiavi, et al., Selective recovery of cobalt from mixed lithium ion battery wastes using deep eutectic solvent, Chem. Eng. J., 417 (**2021**)

[16] Zehui Zhang, Jianghua Qiu, Min Yu, et al., Performance of Al-doped LiNi1/3Co1/3Mn1/3O2 synthesized from spent lithium ion batteries by sol-gel method, Vacuum, 172 (**2020**), 109105–109105, doi:10.1016/j.vacuum.2019.109105

[17] Luo Xu-fang, Xianyou Wang, Li Liao, et al., Effects of synthesis conditions on the structural and electrochemical properties of layered Li[Ni1/3Co1/3Mn1/3]O2 cathode material via the hydroxide co-precipitation method, LIB SCITECH, Journal of Power Sources, 161 (**2006**), 601–605, doi:10.1016/j.jpowsour.2006.03.090

[18] Luqi Zhuang, Conghao Sun, Tao Zhou, et al., Recovery of valuable metals from LiNi0.5Co0.2Mn0.3O2 cathode materials of spent Li-ion batteries using mild mixed acid as leachant, Waste Management, 85 (**2019**), 175–185, doi:10.1016/j.wasman.2018.12.034

[19] Tlek Ketegenov, Kaster Kamunur, Lyazzat Mussapyrova, et al., Enhanced Recovery of Lithium and Cobalt from Spent Lithium-Ion Batteries Using Ultrasound-Assisted Deep Eutectic Solvent Leaching, Metals, 14 (**2024**) 9, 1052, doi:10.3390/met14091052

[20] Pier Giorgio Schiavi, Pietro Altimari, Mario Branchi, et al., Selective recovery of cobalt from mixed lithium ion battery wastes using deep eutectic solvent, Chemical Engineering Journal, 417 (**2021**), 129249, doi:10.1016/j.cej.2021.129249

[21] Yi Luo, Leming Ou, Chengzhe Yin, High-efficiency recycling of spent lithium-ion batteries: A double closed-loop process, Science of The Total Environment, 875 (**2023**), 162567, doi:10.1016/j.scitotenv.2023.162567